Manuscript

FLAW IMPULSE RESPONSE ESTIMATION IN ULTRASONIC NONDESTRUCTIVE EVALUATION USING BI-CEPSTRA

A. Yamani
K.F.U.P.M. Box 1811
Dhahran 31261, Saudi Arabia
email: myamani@dpc.kfupm.edu.sa

ABSTRACT

Pulse echo measurements in ultrasonic nondestructive evaluation (NDE) are masked by the characteristics of the measuring instruments, the propagation paths taken by the ultrasonic pulses, and are considered to be corrupted by additive noise. It is assumed that the measured pulse echo is obtained by linearly convolving the defect impulse response (IR) with the measurement system response. Deconvolution operation therefore, seeks to undo the effect of this convolution and extract the IR which is essential for defect identification. Autocorrelation (or power spectrum) deconvolution techniques are limited to the identification of minimum phase systems. In this work, we show that higher order cepstra can be used to deconvolve the IR of the flaw from ultrasonic echo measurements (synthetic as well as real). We also demonstrate that a deconvolution based on the use of the bicepstrum gives lower identification error variance when compared with the results of Wiener filtering deconvolution, specially at low signal-to-noise ratios (SNR).

Keywords: cumuland, deconvolution, HOS, pulse –echo, impulse response.

1. Introduction

In a typical ultrasonic inspection system, ultrasonic pulses are generated by a piezoelectric transducer coupled to the test specimen. As the ultrasonic wave propagates through the material, some of its energy will be reflected whenever it encounters in its path an inhomogeneity, a discontinuity, or the back surface of the specimen. The reflection (echos) are then measured using a pulser-receiver [1]. If the velocity of the ultrasonic wave in the tested material has previously been determined, then from a measurement of the round trip travel time, the distance between the transducer and the defect can be deduced. However, this information alone is not sufficient for many of today's highly sophisticated manufacturing processes. In many cases, the geometry of the hidden defect is of interest [2]. For example, some ultrasonic reflectors (e.g. planar cracks) are much more likely to lead to eventual failure than volumic flaws such as slag or porosity. In ultrasonic NDE of materials, it is considered that pulse echo measurements are masked by the characteristics of the measuring instruments, the propagation paths taken by the ultrasonic pulses, and are considered to be corrupted by additive noise. It is assumed that the measured pulse echo is obtained by linearly convolving the defect IR with the measurement system response. Deconvolution operation therefore, seeks to undo the effect of this convolution and extract the IR which is essential for defect identification.

The problem of deconvolution have many applications in areas such as communications, seismology, and medical imaging. Chen [2] has applied different deconvolution techniques to ultrasonic NDE, and it seem from his study that Wiener filtering produces acceptable results. There are however some drawbacks to Wiener as well as to other SOS-based deconvolution techniques, which are their inability to accurately identify non-

minimum phase systems, and their accuracy depends upon a priori knowledge of the noise statistics. Some of these deconvolution techniques such as Wiener filtering, and spectral extrapolation are based on a priori knowledge of second-order statistics (SOS) of the noise and the input signal which is not available in many cases. SOS based deconvolution techniques such as the least squared error (L_2), the L_1 and Wiener give poor results at low SNR. In addition, (L_2), the L_1, in particular, are sensitive to time shifts in the measurement signal with reference to the input signal. Thus they require signal alignment prior to processing. Moreover, ultrasonic pulse echoes can be of minimum or non-minimum phase systems. SOS-based deconvolution techniques, being phase blind, are not expected to accurately identify the defect impulse response in the case of non-minimum phase [3].

In this work we process the data in the poly-cepstra domain which is more suitable to eliminate effects of any additive Gaussian noise, and identify both minimum and non-minimum phase systems [4]. Without loss of generality, we show examples using the bi-cepstrum. We apply the proposed technique to simulated as well as real ultrasonic signals and compare it with those obtained using Wiener filtering.

2. Higher-Order Statistic Approach

Higher-order statistics (HOS); also known as cumulants, of a random process are related to its joint moments [3]. They give a measure of the distance of the random process from Gaussianity. This can easily be seen from the definition of the nth order cumulant of the zero-mean stationary random process $w(k)$ given as

$$c_n^w(k_1,k_2,\cdots,k_{n-1}) = E\{w(k_1)\cdots w(k_{n-1})\} - E\{g(k_1)\cdots g(k_{n-1})\} \qquad (1)$$

where $g(k)$ is a zeros-mean Gaussian random process having the same variance as $w(k)$ [4], and $E\{\}$ is the statistical expectation operator. Related to the cumulants are the poly-spectra, and poly-cepstra. The z-transform of the nth order cumulant produces the nth order spectrum. Whereas the nth order cepstrum is obtained from the inverse z-transform of its corresponding log spectrum. Therefore, the bi-cepstrum of a non Guassian random process $y(k)$ can be written as

$$v_3^y(k_1, k_2) = Z^{-1}\left\{\ln\left[C_3^y(z_1, z_2)\right]\right\} \tag{2}$$

where Z^{-1} is the inverse z-transform, and

$$C_3^y(z_1, z_2) = Z\left\{\left[c_3^y(k_1, k_2)\right]\right\} \tag{3}$$

3. Problem Formulation

It is assumed that a defect is modeled as a linear time-invariant (LTI) system such that it is characterized by its corresponding "impulse response", $h(t)$. Assuming a linear convolution model for the ultrasonic flaw signal such as

$$y(k) = x(k) \otimes h(k) + n(k) \tag{4}$$

where $x(k)$ is the flawless reference signal, $h(k)$ is the flaw's impulse response, and $n(k)$ is an additive Gaussian white noise (AGWN). Our task is to extract the flaw's impulse response $h(k)$ from Equ.(4) from measurements of $y(k)$, and $x(k)$.

Since the poly-spectrum of AGWN is zero, then the noise-free bi-spectrum of Equ.(4) is given by

$$C_3^y(z_1, z_2) = C_3^x(z_1, z_2) C_3^h(z_1, z_2) \tag{5}$$

which shows that the use of HOS-based deconvolution techniques, alleviates the effect of the additive noise. In addition, it enables us to identify both minimum and non-minimum phase systems. It is found [5,6] that the finite bi-cepstral parameters A_i's and B_i's, computed from equ.(5), can be used in the recursion

$$h_{\min}(k) = -\frac{1}{k} \sum_{i=2}^{k+1} A_{i+1} h_{\min}(k-i+1); \quad k \geq 1 \tag{6a}$$

$$h_{\max}(k) = \frac{1}{k} \sum_{i=k+1}^{0} B_{i+1} h_{\max}(k-i+1); \quad k \leq 1 \tag{6b}$$

where $h_{\min}$ and $h_{\max}$ are respectively the minimum-phase and non-minimum-phase components of the system impulse response $h(t)$ given by

$$h(k) = h_{\min}(k) \otimes h_{\max}(k) \tag{7}$$

The identified system impulse response obtained using the bi-cepstral parameters is based on a system driven by a non Gaussian white noise input. Since the available reference signal $x(t)$, is not necessarily white, thus, a pre-whitening filter for $x(t)$ is used as shown in Fig. 1.

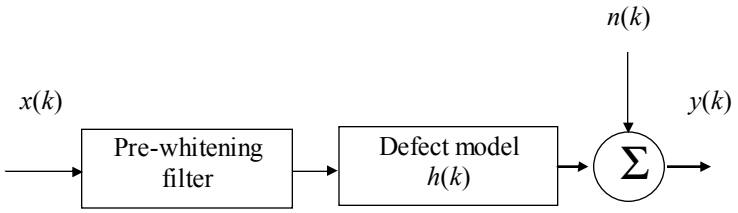

Figure 1. The model used in the identification of the defect's impulse response

4. Tests

4.1 simulations

The synthesized data is generated as follow. The input $x(t)$ used for the defect model shown in Fig. 1 is produced using a sinusoidal signal with frequency in the ultrasonic range, that amplitude modulates a Gaussian pulse. The noise, $n(t)$ is Gaussian white with zero mean and variance σ which is varied in order to obtain different signal-to-noise ratios (SNR). The defect is represented by three different LTI systems to cover all practical parametric modeling, namely an autoregressive (AR), a moving average (MA), and an autoregressive moving average (ARMA) systems. Simulated pulse echo data for each model is thus generated by equ.(4), with different SNRs.

The three models considered are:

a) A minimum phase autoregressive (AR) system whose transfer function is given by

$$H_{AR}(z) = \frac{1}{1 - 0.7z^{-1} + 0.6z^{-2} - 0.3z^{-3}} \qquad (8).$$

b) A non minimum phase moving average (MA) system whose transfer function is given by

$$H_{MA}(z) = z^2 - 3.4001z + 2.7697 + 0.6978z^{-1} \qquad (9).$$

c) A non minimum phase autoregressive moving average (ARMA) system whose transfer function is given by

$$H_{ARMA}(z) = \frac{1 - 3.25z^{-1} + 3.5399z^{-2} - 1.2487z^{-3}}{1 - 1.86z^{-1} + 1.47z^{-2} - 0.5246z^{-3}} \qquad (10).$$

In this section, the bi-cepstral deconvolution technique is first tested on synthesized data. The bi-spectra of *x(t)* and *y(t)* are calculated first, and used to compute the bi-cepstral parameters using the relationship defined by Pan and Nikias [5]. Then, the defect impulse response is estimated using these bi-cepstral parameters as in Equs.(6) and (7). The estimation error

variances between the actual and the estimated impulse responses is then calculated for different SNR.

In order to compare SOS with its counterpart HOS deconvolutions, the minimum-phase AR system is considered first and the system IR is estimated using both Wiener Filter (SOS) and the proposed bi-cepstrum deconvolution (HOS). Although Wiener filter is expected to accurately produce the minimum-phase system IR, it can be seen from Fig.2 that the proposed technique outperforms conventional deconvolution methods especially at low SNR.

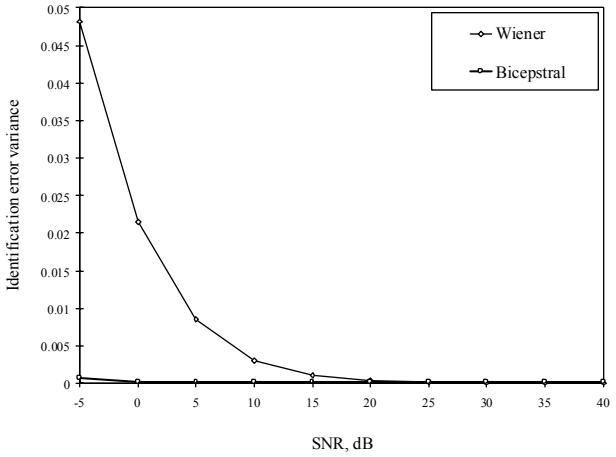

Figure 2. Estimation Error variances of the AR system impulse response.

To appreciate the effect of the estimation error variance on the computed IR, both theoretical (actual) and estimated IR signals using Wiener and Bi-cepstrum techniques are shown in Fig.3 (a) and (b) respectively at SNR=5 dB. Although the estimation error variance for Wiener filter is about 1% at SNR of 5dB, it can be seen that the resultant IR has pronounced oscillations which may result in an erroneous defect classification that is based on time-domain feature.

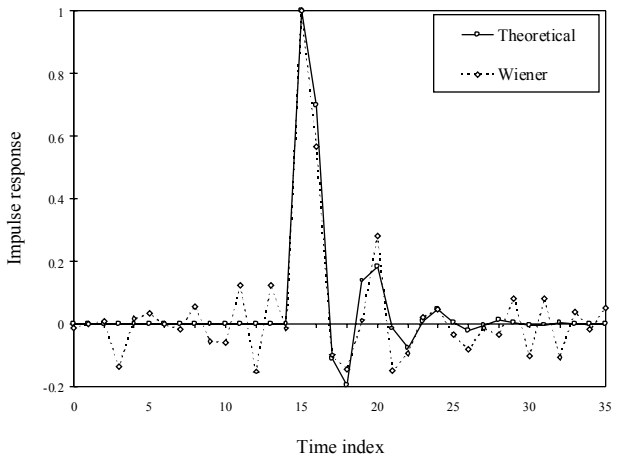

(a)

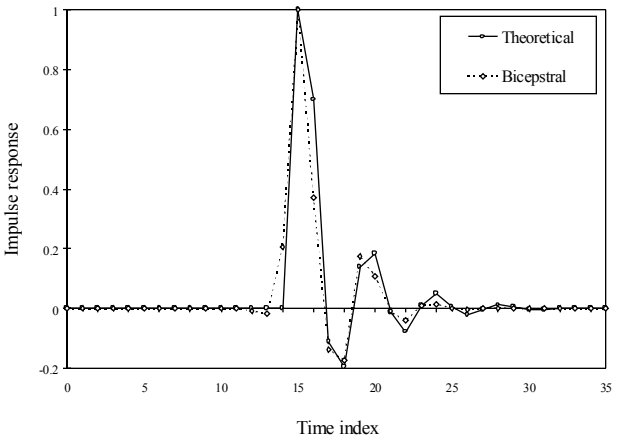

(b)

Figure 3. Impulse responses of the AR system obtained from a) Wiener filtering technique, b) bicepstral deconvolution technique. For SNR=5 dB.

Next, maximum-phase systems (MA and ARMA) are considered. Wiener filter fails to estimate accurate IR and thus, it is not included here. However, when the proposed technique

is used, highly accurate estimation is obtained for both systems at an SNR as low as 5 dB. This is shown in Fig. 4 for MA system and in Fig. 5 for ARMA system.

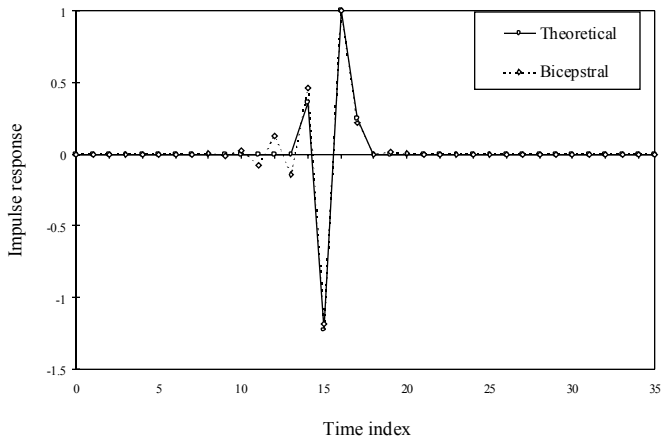

Figure 4. Theoretical and estimated impulse responses of the MA system (at SNR=5 dB).

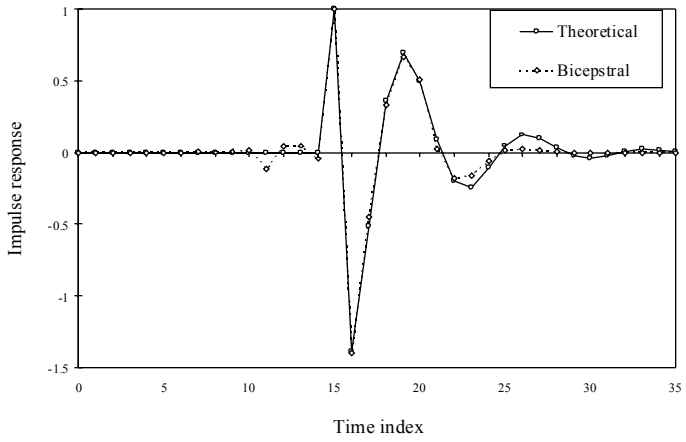

Figure 5. ARMA system impulse response : true and estimated impulse responses for a SNR=5 dB.

4.1 Real ultrasonic data

The proposed bicepstrum deconvolution technique is tested on the real ultrasonic data used in [2]. The reference signal A0 obtained from the flawless sample is used as a reference to deconvolve each flaw IR from its corresponding pulse echo measurements. Two artificial defects are considered; namely an angular-cut hole (A2), and a circular-cut hole (A3), in aluminum blocks, (see [2] for an illustration of these defect geometries). The center frequency of the transducer used is 15 MHz, and the A-scan signals contain 512 data points digitized at a rate of 100 MHz. The pulse-echo signals corresponding to A0, A2, and A3 samples are represented by T15A0, T15A2, and T15A3 respectively. For illustration, the signals T15A2 and T15A3 are shown in Fig. 6 and Fig.7 respectively.

When the bicepstrum-based deconvolution technique is applied to real ultrasonic signals, namely, T15A2 and T15A3, with T15A0 taken as the reference signal, smooth, oscillation-free impulse responses (compared to other conventional deconvolution techniques as in [2]) are obtained as shown in Figs. 8 and 9.

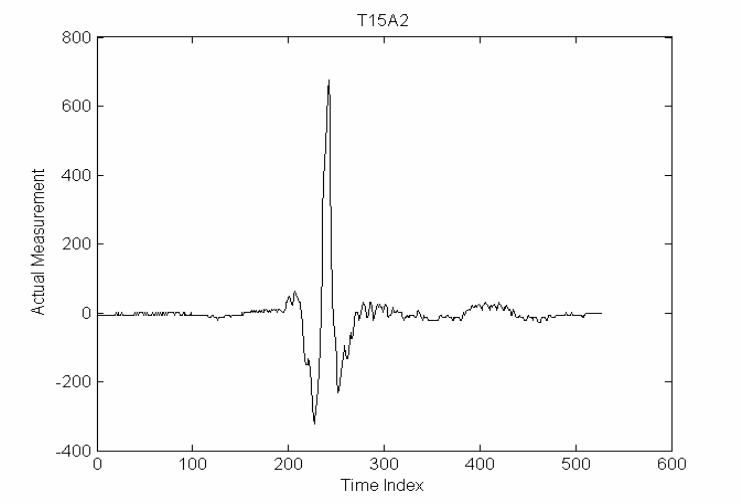

Figure 6. Actual ultrasonic pulse echo for the angular-cut specimen (A2).

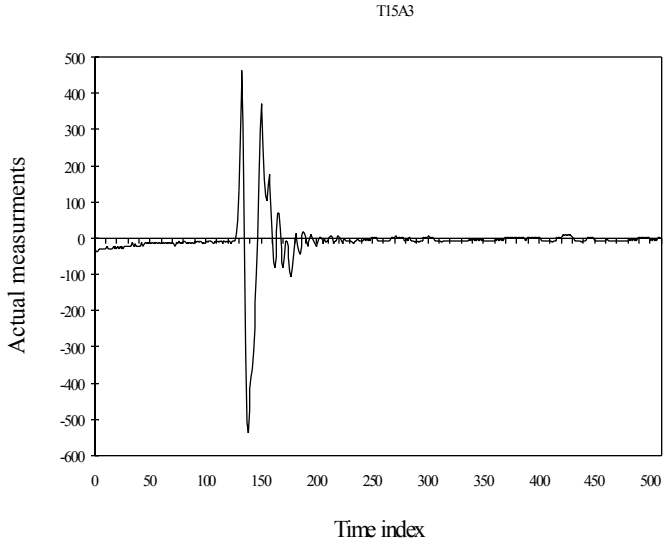

Figure 7. Actual ultrasonic pulse echo for the circular-cut specimen (A3).

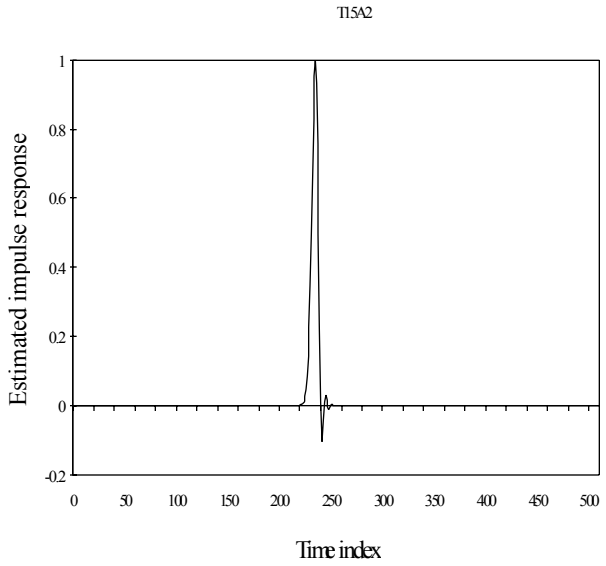

Figure 8. Impulse response of the angular-cut hole (A2).

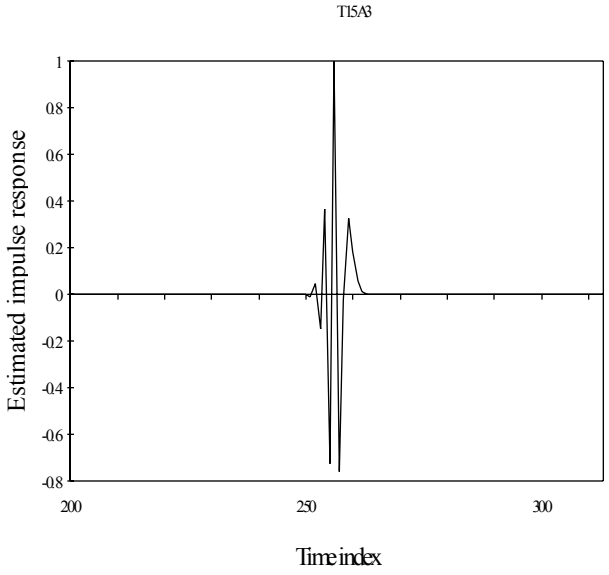

Figure 9. Impulse response of the circular-cut hole (A3).

CONCLUSION

We have shown that higher order cepstrum can be used in the identification of flaws impulse responses in ultrasonic evaluation. It has been demonstrated that the effects of AWGN can be eliminated. In addition, identification of both minimum and nonminimum phase IR is possible. In our future work we intend to study the affect of non Gaussian additive noise on the results of flaw impulse response identification using polycepstra as well as polyspectra.

ACKNOWLEDGMENT

The authors would like to thank KFUPM for the research facilities provided to accomplish this work.

REFERENCES

1. A. Abbate, J. Koay, J. Frankel, S. C. Schroader, and P. Das, "Signal detection and noise suppression using a wavelet transform signal processor: Application to ultrasonic flaw detection", IEEE trans. On Ultrason., Ferroelect., and Freq. Contr., vol. 44, pp. 14-25, 1997.
2. C. H. Chen, and S. K. Sin, "On effective spectrum-based ultrasonic deconvolution techniques for hidden flaw characterization", J. accoust. Am. 87 (3), pp. 976-987, 1990.
3. C. L. Nikias, and M. R. Raghuveer, "Bispectrum estimation: A digital signal processing framework", Proc. IEEE, vol. 75, no. 7, pp. 869-891, 1987.
4. J. M. Mendel, "Tutorial on higher-order statistics (spectra) in signal processing and systems theory: Theoretical results and some applications", Proc. IEEE, vol. 79, no. 3, pp. 278-305, 1991.
5. R. Pan, and C. L. Nikias, " The complex cepstrum of higher-order cumulants and non minimum phase system identification", IEEE Trans. On ASSP, vol. 36, no. 2, pp. 185-205, Feb. 1988.
6. C. L. Nikias, and A. P. Petropulu, *High-order spectra analysis: A nonlinear signal processing framework*, Prentice Hall, Englewood Cliffs, NJ, 1993.